Angewandte Chemie International Edition

Angewandte International Edition Chemie

GDCh German Chemical Society

How to cite: *Angew. Chem. Int. Ed.* **2026**, e8143908
doi.org/10.1002/anie.8143908

COMMUNICATION

Tune, Extend, and Narrow the Useful Dynamic Range of Cell-Free Transcription Biosensors Through Programmable DNA-Based Stem-Loop Hairpin Reporters

João M. R. Aguiar[1] | Sara Bracaglia[1] | Simona Ranallo[1] | Francesco Ricci[1,2]

[1]Department of Chemical Sciences and Technologies, University of Rome, Rome, Italy | [2]Istituto Nazionale Biostrutture e Biosistemi (INBB), Rome, Italy

Correspondence: Simona Ranallo (simona.ranallo@uniroma2.it) | Francesco Ricci (francesco.ricci@uniroma2.it)

Received: 22 December 2025 | **Revised:** 7 April 2026 | **Accepted:** 13 April 2026

Keywords: cell-free biosensors | cell-free reporters | cell-free synthetic biology | dynamic range

ABSTRACT

In this work, we present a general, modular strategy to tune, extend, and narrow the dynamic range of cell-free transcription biosensing platforms by integrating programmable, structure-switching DNA stem-loop reporters into in vitro transcription (IVT) circuits. To do so, we engineered a set of stem-loop DNA reporters whose dynamic range for detecting a specific RNA output can be precisely controlled by adjusting their switching equilibrium constant (K_S). This straightforward approach enables the dynamic range of a model cell-free transcription biosensor to be programmed across more than two orders of magnitude (observed affinity K_D^{obs} from 0.16 ± 0.02 nM up to 23 ± 4 nM). By combining DNA-based reporters with differing affinities, we further expanded the dynamic range of a cell-free transcription biosensor well beyond the conventional two orders of magnitude, achieving up to 10^4-fold coverage. We also demonstrate two-step dynamic responses by mixing hairpin reporters with highly distinct affinities. Finally, integration of signaling and non-signaling stem-loop reporters allowed us to compress the dynamic range of a model transcription biosensor to as little as three-fold enabling heightened sensitivity. Overall, this modular framework enables the customization of cell-free transcription biosensor sensitivity and response profiles, overcoming key limitations inherent to single-site transcriptional reporter designs.

1 | Introduction

Cell-free transcription (also known as in vitro transcription or IVT), a growing field within synthetic biology [1, 2] allows the recreation of transcription outside cells by using core transcriptional components (such as RNA polymerases and nucleotides) and synthetic DNA templates to rapidly produce an RNA sequence of interest in vitro with high yield [3]. Cell-free transcription has found many applications in biosensing, as responsive DNA templates can be designed to rapidly transduce target recognition into a detectable transcriptional RNA output [4–6]. Recent examples of cell-free transcription biosensors have demonstrated the sensitive detection of clinically relevant protein biomarkers [4], water contaminants like metal ions [6], small molecules and antibiotics, as well as metabolic biomarkers [7]. Cell-free biosensors have also been demonstrated in various immunoassay formats for the detection of antibody/antigen interactions [8–10]. The broad utility of these platforms demonstrates that cell-free transcription offers unprecedented modularity, sensitivity, and specificity for sensing technologies.

Cell-free transcription biosensors currently use almost exclusively two types of reporters: fluorescent light-up RNA aptamers [6, 7, 9] such as the mango aptamer [11] and strand-displacement probes [4, 12]. Light-up aptamers are RNA sequences evolved to bind a fluorogen with high affinity and activate its fluorescence

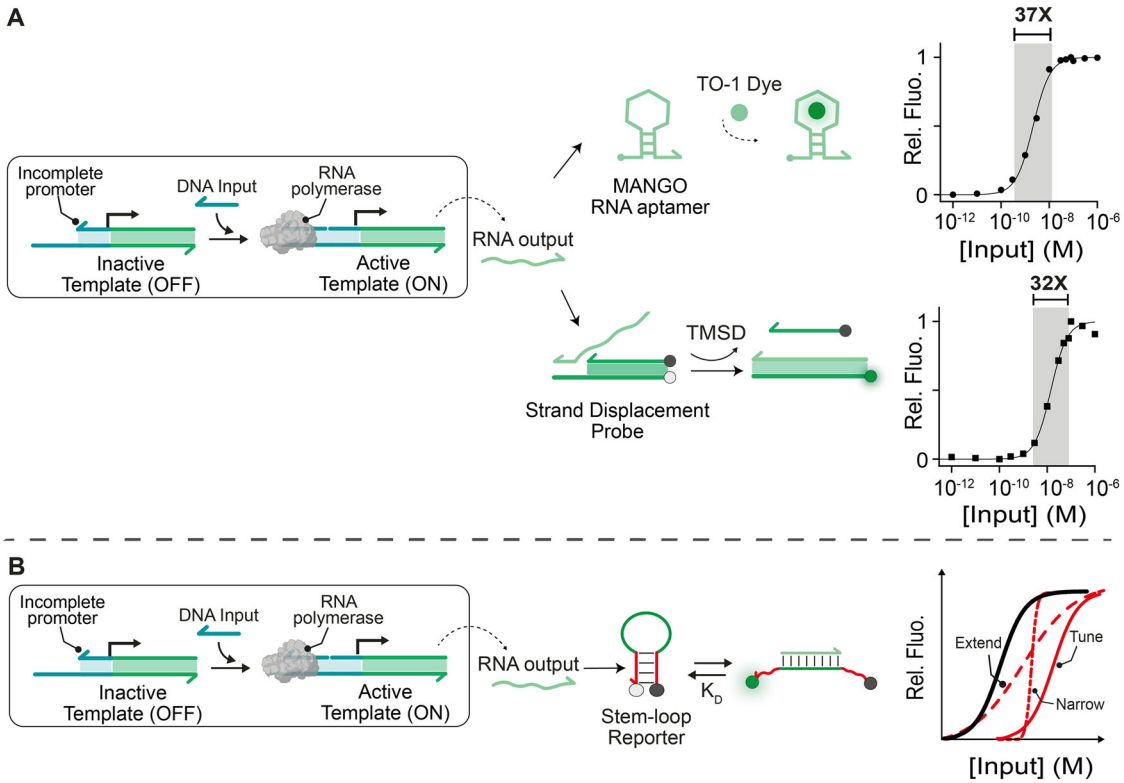

FIGURE 1 | (A) Two model cell-free transcription biosensor examples employing templates encoding either a Mango RNA light-up aptamer, or an RNA strand inducing a toehold-mediated strand displacement reaction (TMSD) of a fluorophore-quencher labelled DNA duplex probe were used to determine the useful dynamic range of typical cell-free transcription biosensors. Binding curves were performed by providing increasing concentrations of target input enabling higher transcription yields. The dynamic range of the model cell-free biosensors (target concentration corresponding to 10%–90% fluorescence signal transition) was 37- and 32-folds, respectively, close to the expected theoretical 81-fold of single-site binding systems. In both cases, the IVTx reactions were performed in a 25 uL buffer solution (HEPES 40 mM, $MgCl_2$ 50 mM, spermidine 1 mM, Triton 100× 0,01%, PEG 4%, DTT 5 mM) containing the inactive transcription template (100 nM), T7 RNA polymerase (5 U/μL), RiboLock RNase Inhibitor (1 U/μL) and nucleoside triphosphate (NTPs) mix (10 mM) and as reporters either the Thiozole Orange 1 or T0-1Dye (200 nM) for the Mango aptamer or a DNA duplex labelled with a fluorophore(6-FAM)/quencher(BHQ-1) probe (300 nM). The DNA input strand was added at different concentrations from 10 pM up to 1 μM, and endpoint fluorescence signals were measured after 2 h at 37°C. The error bars correspond to the standard deviation of three independent replicate measurements. (B) Outline of strategies envisioned to program the dynamic range (DR) of cell-free biosensors. A transcription template produces an RNA output in response to the presence of a target input, which is then detected by a DNA-based reporter consisting of a stem-loop hairpin modified with a fluorophore/quencher moiety. Using different combinations of stem-loop reporters/depletants with varying affinities for the same RNA output strand, we can tune, extend, or narrow at will the dynamic range of cell-free biosensors' response.

[13], while strand-displacement probes consist of a DNA duplex modified with fluorophore/quencher moieties [12] that, upon toehold-mediated strand displacement reaction (TMSD) induced by the RNA transcribed strand, are separated leading to a signal increase [12]. Although both strategies are robust, their reliance on single-site biomolecular recognition imposes an intrinsic limitation on dynamic range, dictated by biophysical binding properties and commonly modelled by a hyperbolic (Langmuir) response. This results in a useful dynamic range (defined here as the concentration range where a sensor produces a detectable and proportionally changing signal, from 10% to 90% of its maximum signal change) that spans approximately 81-fold [14, 15], which may be insufficient for diverse diagnostic needs—for example, where the biological window is much broader (as in viral load monitoring) [16] or narrower (as in metabolite or drug threshold-based decisions) (Figure 1A) [17].

Faced with a similar limitation (i.e., the fixed dynamic range of single-site binding), nature has evolved multiple strategies to extend or narrow the effective response window of receptors. These include cooperative (allosteric) binding, the use of multiple receptors with varying affinities and sequestration by high-affinity non-signaling "depletant" molecules [15, 18–22]. These design principles have recently inspired rational tuning of dynamic ranges in both DNA and protein-based sensor platforms [23–25]. Increasingly, analogous approaches are also being adapted for cell-free transcription biosensors, albeit in a limited scope. Notable examples include programmable target affinity templates and engineered template circuits [5]. Recently, Lucks and colleagues also showcased strand displacement probes with varied transcript target affinities to build an analogue-to-digital converter (ADC) circuits in genetic systems [12]. In another application, a similar digital-like behavior was achieved by Schulman and colleagues by coupling their dART biosensors with comparator circuits [4]. Despite these advances, the development of broadly applicable and programmable methods to dynamically modulate the sensing range of cell-free transcription biosensors remains an open and important challenge.

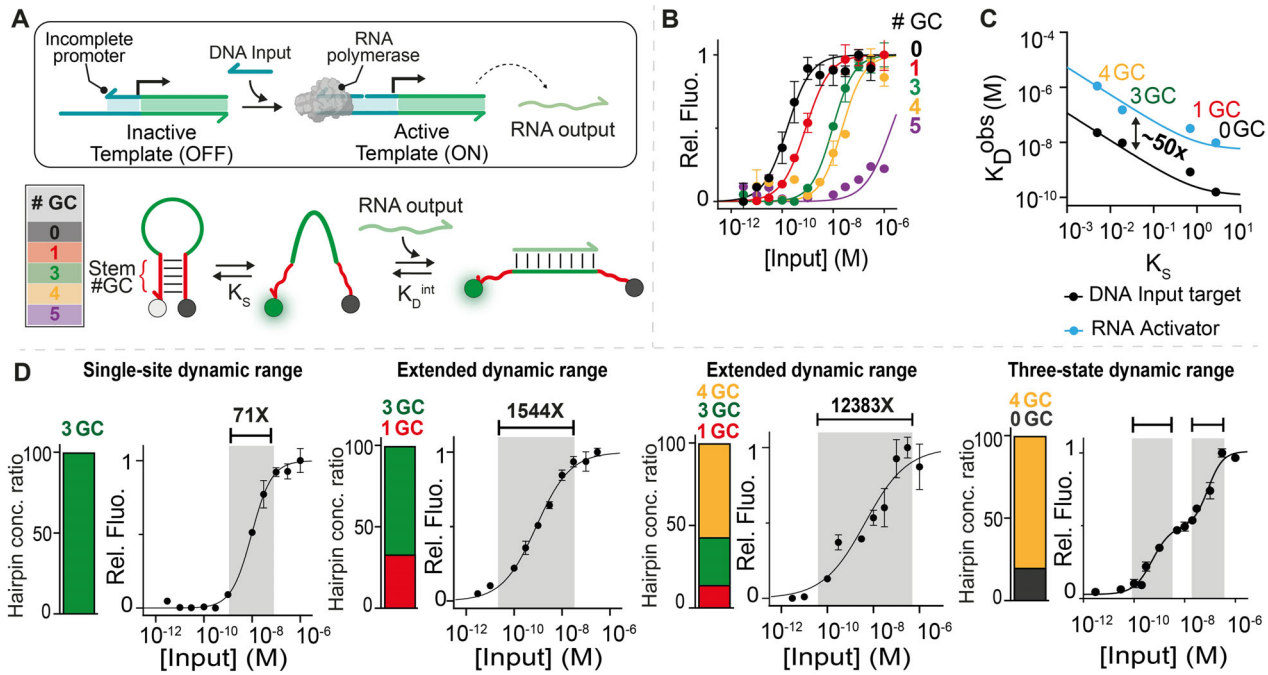

FIGURE 2 | Extending the dynamic range (DR) of cell-free biosensors. (A) In the presence of a specific DNA input strand (our target), the inactive DNA template can be activated to enable IVT and produce an RNA output strand that can then bind to a stem-loop hairpin reporter modified with a fluorophore/quencher pair leading to a fluorescent signal increase. Five reporter variants with increasing numbers of GC base-pairs in the stem were used (0 GC, 1 GC, 3 GC, 4 GC, and 5 GC). (B) Cell-free transcription binding curves obtained at different concentrations of DNA input strand with the different hairpin reporters. (C) Reporter binding affinity (K_D^{obs}) versus switching equilibrium constant (K_S). As a comparison, the K_D^{obs} (observed affinity) values obtained from binding curves using a synthetic RNA strand ('activator') are also shown. (D) Cell-free transcription binding curves obtained at different concentrations of DNA input strand using a mix of two or three hairpin reporters with different affinities. The histogram plot shows the concentration ratio of the hairpin reporters used in each experiment. In this and in the following figures, the cell-free transcription reaction was performed in a 25 µL buffer solution (HEPES 40 mM, $MgCl_2$ 50 mM, spermidine 1 mM, Triton 100× 0,01%, PEG 4%, DTT 5 mM) containing the inactive template (100 nM), T7 RNA polymerase (5 U/µL), RiboLock RNase Inhibitor (1 U/µL), nucleoside triphosphate (NTPs) mix (10 mM) and different concentrations of the DNA input strand (from 10 pM to 300 nM). The reaction was allowed to proceed for 120 min at 37°C and an aliquot was transferred into a sodium phosphate buffer solution containing the relevant hairpin reporter and endpoint fluorescence signal was recorded after 30 min. The error bars correspond to the standard deviation of three independent replicate measurements.

Motivated by the above considerations, the present work proposes a generalizable approach: the design and combined implementation of programmable, affinity-tuned stem-loop DNA reporters in cell-free transcription biosensors. Stem-loop hairpins modified with fluorophore/quencher groups have seen limited applications in IVT systems [26], especially as biosensor reporting systems, but are especially useful for dynamic range modulation applications since their target affinity can be rationally and easily tuned without changing their target specificity [27]. By mixing such reporters with distinct affinities, it is possible to tailor, expand, or narrow (Figure 1B) the cell-free transcription sensor's dynamic range and thereby overcome the intrinsic limitations imposed by conventional single-site reporter binding.

2 | Results and Discussions

In this work, we have employed as a model cell-free transcription biosensor a transcription template composed of two complementary DNA strands that form a coding domain and an incomplete T7 RNA polymerase (T7 RNAP) promoter domain (Figure 2A). Because the promoter is truncated on its template strand, transcription by T7 RNAP does not occur unless a linear input strand (our target), which completes the promoter sequence, is added. Upon input binding, a functional promoter is reconstituted, and a short 19-nt RNA output strand is transcribed. In common cell-free transcription biosensors, either a light-up aptamer is transcribed, or a duplex reporter is used to detect the RNA output [7, 12]. In both cases, however, the dynamic range observed is usually less than two orders of magnitude and cannot be easily tuned at will. We demonstrate this experimentally with our model cell-free transcription biosensor showing that the dynamic range observed with a light-up RNA aptamer and a strand displacement reporter covers, respectively, 37- and 32-folds of DNA input concentration (see Figure 1A). To achieve programmable modulation of the dynamic range of this model cell-free transcription biosensor, we have used here a DNA-based stem-loop hairpin reporter (Figure 2A, bottom) modified with a fluorophore/quencher pair at the two ends and displaying a 13-nt loop designed for specific hybridization to the RNA output strand and a 5 base-pair stem formed by self-complementary bases [28, 29]. In the absence of the RNA output strand, the reporter predominantly adopts a non-emissive conformation (closed loop), with the fluorophore quenched. RNA output binding to the loop destabilizes the stem, inducing the structure to adopt an open, emissive state in which the fluorophore and quencher are separated, resulting in a robust fluorescence signal increase [30, 31]. This conformational change is governed by the hairpin's switching equilibrium, which can

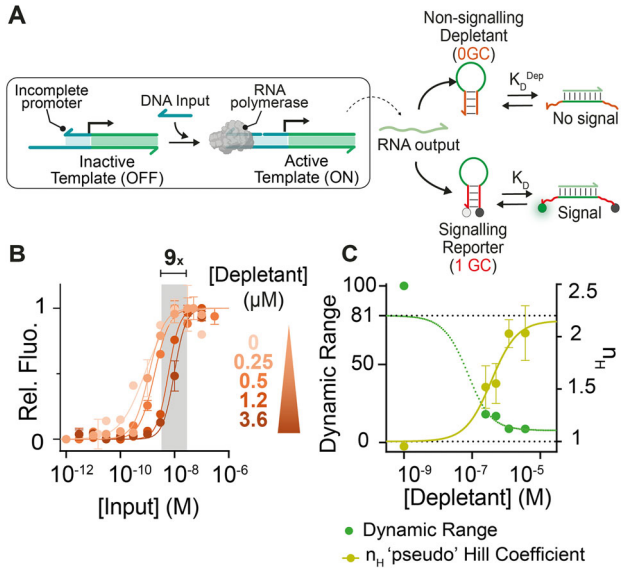

FIGURE 3 | Narrowing the dynamic range (DR) of cell-free biosensors. (A) The reporter system is composed of a high-affinity non-signaling (i.e., depletant) and a lower-affinity signaling reporter (1 GC). (B) Cell-free transcription binding curves obtained at different concentrations of the depletant (from 250 nM to 3.6 μM) and a fixed concentration of signaling reporter (5 nM). (C) 'Pseudo'-hill coefficients and dynamic range fold change versus depletant concentration used for all cell-free transcription binding curves. The error bars correspond to the standard deviation of three independent replicate measurements.

be rationally tuned by simply changing the GC content in the stem while maintaining the same loop sequence, thus allowing for precise modulation of the energy barrier (K_S) associated with switching.

As part of our objective to tune the useful dynamic range of cell-free biosensors at will, we set out to build a matched set of reporters with different affinities for the same RNA output transcript [32]. A library of five reporters, each bearing stems with increasing numbers of GC base pairs (from 0 to 5), was designed to systematically span a broad range of switching equilibria and binding affinities (Figure 2A). All reporters retain identical 13-nt loop sequences and thus intrinsic target affinity (K_D^{int}) for the output RNA strand, but their observed affinity (K_D^{obs}) varies due to differences in stem stability modulating conformational switching as predicted by the three-state population-shift model that relates switching thermodynamics to observed binding affinities for similar ligand-induced structure-switching biomolecules [27].

$$K_D^{obs} = K_D^{int}\left(\frac{1+K_s}{K_s}\right) \quad (1)$$

The reporter's K_S, therefore, determines how readily a ligand's binding can shift the equilibrium between the non-emissive and emissive states of the stem-loop reporter. Of note, since K_S (and thus the reporter's affinity for the ligand) is modulated through distal-site mutations on the stem and not through mutations on the loop recognition portion, we ensure that all reporters retain the same specificity for the RNA output. The predicted switching equilibrium constants (K_S) for the five reporters described above, calculated using DNA secondary structure prediction tools [33, 34] (see Supporting Information), ranged from 2.7 (0 GC) to 1×10^{-3} (5 GC). Binding assays performed at increasing concentrations of DNA input strand in a cell-free transcription reaction containing the incomplete template and all other core transcriptional components, demonstrated that increasing stem stability (higher GC content) shifts the reporter's dose–response curve to higher input concentrations, corresponding to right-shifted binding curves and K_D^{obs} values ranging from 0.16 ± 0.02 nM up to 23 ± 4 nM for 4 GC reporters (Figure 2B and Table S2). These experimental K_D^{obs} values correlate closely with predicted K_S and accurately fit the three-state population-shift model (Figure 2C, solid line). Additional experiments with the same hairpin reporters but using synthetic RNA strands rather than enzymatic IVT products produced similar trends in K_D modulation (Figures 2C, S1, and Table S2). However, lack of amplification in the direct RNA system resulted in K_D^{obs} values shifted almost two orders of magnitude higher, highlighting the impact of the transcription enzymatic processes on the detection sensitivity of cell-free transcription biosensors (Figures 2C, S1, and Table S2). In addition to that, we also note that stem-loop reporters, as expected, undergo rapid hybridization reactions with their synthetic RNA targets (Figure S2) and thus the overall response kinetics in cell-free transcription reactions is largely governed by transcription kinetics rather than reporter opening. Single hairpin reporters with varied K_S allow the dynamic range to be shifted across distinct concentration regimes, but the absolute span remains largely fixed to about two orders of magnitude due to intrinsic biophysical constraints given by single-site binding [14]. As an example, the dynamic range of the 3 GC hairpin reporter spans 71-fold of DNA input concentration (Figure 2D, left). To achieve the extension of such dynamic range, we thus mixed reporters with different K_S values. For example, combining 1 GC and 3 GC reporters broadened the dynamic range of the cell-free transcription biosensor to over 1500-fold while three-reporter combinations (1 GC, 3 GC, and 4 GC) yielded a log-linear response spanning 10^4-fold change of target concentration (Figure 2D). Combinations with widely spaced affinities (0 GC/4 GC) generated composite two-step response curves for more complex sensing needs (Figure 2D). Of note, in this case the reporters were used in non-equimolar concentrations (see histograms in Figure 2D) to account for the different signal gains of each hairpin reporter.

The availability of reporters with different and programmed affinities for their ligands also enables the narrowing of the dynamic range of our cell-free transcription biosensor. This was accomplished by using high-affinity, non-signaling "depletant" hairpins that sequester the transcript output until saturation, after which any surplus RNA output rapidly triggers a fluorescent hairpin reporter with poorer affinity, producing an ultrasensitive digital-like response analogous to biological sequestration mechanisms [14, 20]. More specifically, as a depletant, we used here the stem-loop hairpin (in this case unlabeled) that provided the highest affinity for the RNA output (i.e., 0 GC) while as the fluorescent reporter we used a stem-loop hairpin with slightly poorer affinity (i.e., 1 GC) (Figure 3A). Dose–response curves were fitted using Hill equation (see Supporting Information) that allows to easily quantify ultrasensitivity in binding assays through the extrapolation of the Hill coefficient [14]. As expected [14, 23, 24], we observed that increasing depletant concentrations from 250 nM to 3.6 μM resulted in a more digital-like response of our

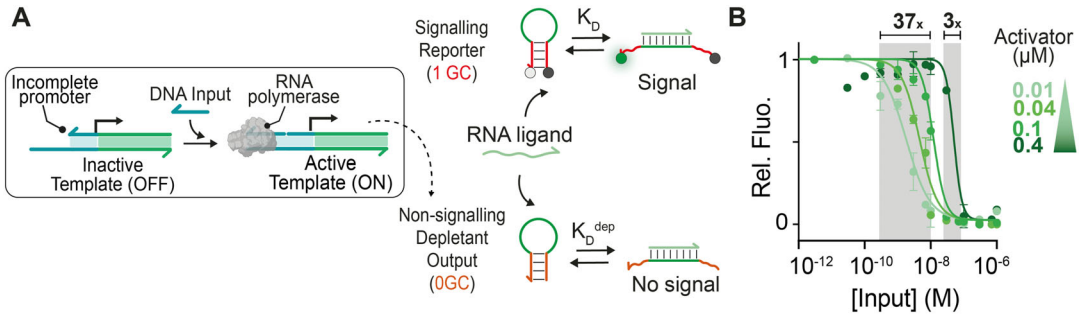

FIGURE 4 | Narrowing the dynamic range (DR) of cell-free biosensors. (A) In this case, the reporter system is composed of a low-affinity signaling reporter (i.e., 1 GC) and a ligand RNA strand ('Activator'), while the output RNA strand transcribed by the template is a high-affinity depletant probe (i.e., 0 GC). (B) Cell-free transcription binding curves obtained at different concentrations of DNA input strand using a fixed concentration of signaling reporter (5 nM) and varying concentrations of the ligand RNA strand ('Activator') (from 0.01 μM to 0.4 μM). The error bars correspond to the standard deviation of three independent replicate measurements.

cell-free transcription biosensor with dynamic ranges decreasing from 100-fold (dynamic range obtained for 1GC reporter alone) to 9-fold and Hill coefficients going from 0.95 ± 0.2 nM to 2.0 ± 0.3 nM, respectively (Figure 3B,C and Table S3). This, however, is achieved at the cost of shifting the detection limit [14, 23, 24] (here defined as the target concentration resulting in a signal equal to three times the standard deviation of the blank signal) to higher concentration values (i.e., from 0.20 nM to 3.4 nM) (Figure 3C and Table S3). Despite these limitations, sequestration-based strategies remain advantageous in contexts requiring threshold-like behavior or selective detection of targets at concentrations exceeding biologically relevant levels [35].

A similar digital-like response can also be achieved by encoding the depletant within the cell-free transcription biosensor and using as a reporter system an optically-labelled stem-loop probe in combination with its cognate RNA ligand strand (Figure 4A). Performing dose–response curves at increasing concentrations of DNA input strands and fixed concentrations of the stem-loop probe and the cognate RNA ligand strand, we observe digital-like responses with, in this case, a suppression of the signal as at higher input DNA concentrations more depletant can be transcribed leading to a full sequestration of the ligand RNA strand thus preventing the opening of the stem-loop reporter to its emissive conformation (Figure 4B). Also in this case, the digital-like response can be finely tuned by varying the concentration of the ligand RNA strand in the reaction mixture. By doing so, we observed a narrowing of the dynamic range from 37-fold using 0.01 μM of ligand RNA to just 3-fold at 0.4 μM of ligand RNA with an associated increase in the Hill coefficient values and shift of the observed LOD values (Table S4).

3 | Conclusion

The ability to extend or narrow the dynamic range of a cell-free transcription biosensor reporter is an important tool for ensuring effective responses to target concentrations and providing adequate sensitivity. Here, we show how simple dynamic range tuning methodologies based on naturally occurring regulatory mechanisms already applied in other biosensing technologies [23, 24] can also be rationally employed in transcription reporter systems using DNA structure-switching stem-loop hairpins to program (i.e., tune, extend, or narrow) the dynamic range of cell-free transcription biosensors. The proposed strategy is highly versatile and can be easily adapted to tune the dynamic range of cell-free transcription based biosensors for the detection of targets other than nucleic acids, including antibodies and proteins [8–10]. Integrating conformation switching into recognition elements within cell-free transcription biosensors is ideal not only because it enables easy tuning of target affinity, which is essential when optimizing the biosensor's dynamic range, but also because it is a widespread, simple, versatile, and rapidly reversible biomolecular recognition mechanism that can be easily reconfigured for many transduction pathways, such as for example electrochemistry [29].

Acknowledgments

This work was supported by the European Research Council (ERC) (project no. 819160 to F.R.), by Associazione Italiana per la Ricerca sul Cancro (AIRC) (project no. 21965 to F.R.), by Italian Ministry of Research (PRIN 2022, project no. 2022TSB8P7 to F.R.) and by the "PNRR M4C2-Investimento 1.4-CN00000041" financed by NextGenerationEU. J.A. was supported by the MSCA-DN SYNSENSO (G.A. 101072980). S.R. acknowledges funding from the European Research Council (ERC) (project n. 101165168) and from the Italian Ministry of University and Research (Fondo Italiano per la Scienza, FIS2, project no. FIS2-2023-04072).

Conflicts of Interest

The authors declare no conflicts of interest.

Data Availability Statement

The data that support the findings of this study are available from the corresponding author upon reasonable request.

References

1. V. Noireaux and A. P. Liu, "The New Age of Cell-Free Biology," *Annual Review of Biomedical Engineering* 22 (2020): 51–77, https://doi.org/10.1146/annurev-bioeng-092019-111110.

2. A. D. Silverman, A. S. Karim, and M. C. Jewett, "Cell-Free Gene Expression: An Expanded Repertoire of Applications," *Nature Reviews Genetics* 21 (2020): 151–170, https://doi.org/10.1038/s41576-019-0186-3.

3. J. Garamella, R. Marshall, M. Rustad, and V. Noireaux, "The All *E. coli* TX-TL Toolbox 2.0: A Platform for Cell-Free Synthetic Biology," *ACS Synthetic Biology* 5 (2016): 344–355, https://doi.org/10.1021/acssynbio.5b00296.

4. H. Lee, T. Xie, B. Kang, X. Yu, S. W. Schaffter, and R. Schulman, "Plug-and-Play Protein Biosensors Using Aptamer-Regulated In Vitro Transcription," *Nature Communications* 15 (2024): 7973.

5. A. Urosevic, I. Federico, G. Ercolani, A. Idili, and F. Ricci, "Structure-Switching DNA Templates for the Rational and Predictable Control of Cell-Free Transcription," *Preprint, ChemRxiv* (2024), https://doi.org/10.26434/chemrxiv-2024-fn51v-v2.

6. J. K. Jung, K. K. Alam, M. S. Verosloff, et al., "Cell-Free Biosensors for Rapid Detection of Water Contaminants," *Nature Biotechnology* 38 (2020): 1451–1459, https://doi.org/10.1038/s41587-020-0571-7.

7. S. Barthel, L. Brenker, C. Diehl, et al., "In Vitro Transcription-Based Biosensing of Glycolate for Prototyping of a Complex Enzyme Cascade," *Synthetic Biology* 9 (2024): ysae013.

8. F. Miceli, S. Bracaglia, D. Sorrentino, A. Porchetta, S. Ranallo, and F. Ricci, "MAIGRET: A CRISPR-Based Immunoassay That Employs Antibody-Induced Cell-Free Transcription of CRISPR Guide RNA Strands," *Nucleic Acids Research* 53 (2025): gkaf238.

9. A. P. Diaz, S. Bracaglia, S. Ranallo, T. Patino, A. Porchetta, and F. Ricci, "Programmable Cell-Free Transcriptional Switches for Antibody Detection," *Journal of the American Chemical Society* 144 (2022): 5820–5826, https://doi.org/10.1021/jacs.1c11706.

10. S. Bracaglia, S. Ranallo, and F. Ricci, "Electrochemical Cell-Free Biosensors for Antibody Detection," *Angewandte Chemie International Edition* 62 (2023): e202216512.

11. E. V. Dolgosheina, S. C. Y. Jeng, S. S. S. Panchapakesan, et al., "RNA Mango Aptamer-Fluorophore: A Bright, High-Affinity Complex for RNA Labeling and Tracking," *ACS Chemical Biology* 9 (2014): 2412–2420, https://doi.org/10.1021/cb500499x.

12. J. K. Jung, C. M. Archuleta, K. K. Alam, and J. B. Lucks, "Programming Cell-Free Biosensors With DNA Strand Displacement Circuits," *Nature Chemical Biology* 18 (2022): 385–393, https://doi.org/10.1038/s41589-021-00962-9.

13. R. J. Trachman III, N. A. Demeshkina, M. W. L. Lau, et al., "Structural Basis for High-Affinity Fluorophore Binding and Activation by RNA Mango," *Nature Chemical Biology* 13 (2017): 807–813, https://doi.org/10.1038/nchembio.2392.

14. A. Vallée-Bélisle, F. Ricci, and K. W. Plaxco, "Engineering Biosensors With Extended, Narrowed, or Arbitrarily Edited Dynamic Range," *Journal of the American Chemical Society* 134 (2012): 2876–2879, https://doi.org/10.1021/ja209850j.

15. J. Ferrell, "Tripping the Switch Fantastic: How a Protein Kinase Cascade Can Convert Graded Inputs Into Switch-Like Outputs," *Trends in Biochemical Sciences* 21 (1996): 460–466, https://doi.org/10.1016/S0968-0004(96)20026-X.

16. C. C. J. Carpenter, M. A. Fischl, S. M. Hammer, et al., "Antiretroviral Therapy for HIV Infection in 1997 Updated Recommendations of the International AIDS Society-USA Panel," *JAMA* 277 (1997): 1962–1969.

17. H. Gerstein, "Is Glucose a Continuous Risk Factor for Cardiovascular Mortality?," *Diabetes Care* 22 (1999): 659–660, https://doi.org/10.2337/diacare.22.5.659.

18. C.-Y. F. Huang, J. E. Ferrell, and E. Koshland, "Ultrasensitivity in the Mitogen-Activated Protein Kinase Cascade," *Proceedings of the National Academy of Sciences USA* 93 (1996): 10078–10083, https://doi.org/10.1073/pnas.93.19.10078.

19. N. E. Buchler and F. R. Cross, "Protein Sequestration Generates a Flexible Ultrasensitive Response in a Genetic Network," *Molecular Systems Biology* 5 (2009): 272, https://doi.org/10.1038/msb.2009.30.

20. E. Levine, Z. Zhang, T. Kuhlman, and T. Hwa, "Quantitative Characteristics of Gene Regulation by Small RNA," *PLoS Biology* 5 (2007): 1998–2010.

21. K. T. Hughes and K. Mathee, "The Anti-Sigma Factors," *Annual Review of Microbiology* 52 (1998): 231–286, https://doi.org/10.1146/annurev.micro.52.1.231.

22. G. Ortega, A. Chamorro-Garcia, F. Ricci, and K. W. Plaxco, "On the Rational Design of Cooperative Receptors," *Annual Review of Biophysics* 52 (2023): 319–337, https://doi.org/10.1146/annurev-biophys-091222-082247.

23. A. Chamorro-Garcia, C. Parolo, G. Ortega, et al., "The Sequestration Mechanism as a Generalizable Approach to Improve the Sensitivity of Biosensors and Bioassays," *Chemical Science* 13 (2022): 12219–12228, https://doi.org/10.1039/D2SC03901J.

24. B. Wei, J. Zhang, X. Ou, X. Lou, F. Xia, and A. Vallée-Bélisle, "Engineering Biosensors With Dual Programmable Dynamic Ranges," *Analytical Chemistry* 90 (2018): 1506–1510, https://doi.org/10.1021/acs.analchem.7b04852.

25. C. J. Tsai, A. del Sol, and R. Nussinov, "Allostery: Absence of a Change in Shape Does Not Imply That Allostery is Not at Play," *Journal of Molecular Biology* 378 (2008): 1–11, https://doi.org/10.1016/j.jmb.2008.02.034.

26. J. Liu, P. Feldman, and T. D. Y. Chung, "Real-Time Monitoring In Vitro Transcription Using Molecular Beacons," *Analytical Biochemistry* 300 (2002): 40–45, https://doi.org/10.1006/abio.2001.5446.

27. A. Vallée-Bélisle, F. Ricci, and K. W. Plaxco, "Thermodynamic Basis for the Optimization of Binding-Induced Biomolecular Switches and Structure-Switching Biosensors," *PNAS* 106 (2009): 13802–13807, https://doi.org/10.1073/pnas.0904005106.

28. A. Vallée-Bélisle and K. W. Plaxco, "Structure-Switching Biosensors: Inspired by Nature," *Current Opinion in Structural Biology* 20 (2010): 518–526, https://doi.org/10.1016/j.sbi.2010.05.001.

29. D. Kang, A. Vallée-Bélisle, A. Porchetta, K. W. Plaxco, and F. Ricci, "Re-Engineering Electrochemical Biosensors to Narrow or Extend Their Useful Dynamic Range," *Angewandte Chemie International Edition* 51 (2012): 6717–6721.

30. S. Ranallo, M. Rossetti, K. W. Plaxco, A. Vallée-Bélisle, F. Ricci, and A. Modular, "A Modular, DNA-Based Beacon for Single-Step Fluorescence Detection of Antibodies and Other Proteins," *Angewandte Chemie International Edition* 54 (2015): 13412–13416. *Angewandte Chemie* 127 (2015): 13412–13416.

31. A. Chamorro, M. Rossetti, N. Bagheri, and A. Porchetta, *Adv Biochem Eng Biotechnol* (Springer, 2024), 71–106.

32. S. Bhattacharya, C. G. Bunick, and W. J. Chazin, "Target Selectivity in EF-Hand Calcium Binding Proteins," *Biochimica et Biophysica Acta (BBA) - Molecular Cell Research* 1742 (2004): 69–79, https://doi.org/10.1016/j.bbamcr.2004.09.002.

33. R. Owczarzy, A. V. Tataurov, Y. Wu, et al., "IDT SciTools: A Suite for Analysis and Design of Nucleic Acid Oligomers," *Nucleic Acids Research* 36 (2008): W163–W169, https://doi.org/10.1093/nar/gkn198.

34. J. N. Zadeh, C. D. Steenberg, J. S. Bois, et al., "NUPACK: Analysis and Design of Nucleic Acid Systems," *Journal of Computational Chemistry* 32 (2011): 170–173, https://doi.org/10.1002/jcc.21596.

35. N. A. Emmons, Z. Duman, M. K. Erdal, J. Hespanha, T. E. Kippin, and K. W. Plaxco, "Feedback Control Over Plasma Drug Concentrations Achieves Rapid and Accurate Control Over Solid-Tissue Drug Concentrations," *ACS Pharmacology & Translational Science* 8, no. 5 (2025): 1416–1423.

Supporting Information

Additional supporting information can be found online in the Supporting Information section.

Material and methods, sequences of nucleic acids, and figures can be found in the Supporting Information.

Supporting file 1: anie72333-sup-0001-SuppMat.docx.